Neutron Capture and the Antineutrino Yield from Nuclear Reactors

Patrick Huber* and Patrick Jaffke†
Center for Neutrino Physics, Virginia Tech, Blacksburg, Virginia 24061, USA
(Received 9 November 2015; published 24 March 2016)

We identify a new, flux-dependent correction to the antineutrino spectrum as produced in nuclear reactors. The abundance of certain nuclides, whose decay chains produce antineutrinos above the threshold for inverse beta decay, has a nonlinear dependence on the neutron flux, unlike the vast majority of antineutrino producing nuclides, whose decay rate is directly related to the fission rate. We have identified four of these so-called nonlinear nuclides and determined that they result in an antineutrino excess at low energies below 3.2 MeV, dependent on the reactor thermal neutron flux. We develop an analytic model for the size of the correction and compare it to the results of detailed reactor simulations for various real existing reactors, spanning 3 orders of magnitude in neutron flux. In a typical pressurized water reactor the resulting correction can reach ∼0.9% of the low energy flux which is comparable in size to other, known low-energy corrections from spent nuclear fuel and the nonequilibrium correction. For naval reactors the nonlinear correction may reach the 5% level by the end of cycle.

DOI: 10.1103/PhysRevLett.116.122503

Science with antineutrinos and nuclear reactors have been intimately connected since the discovery of the antineutrino by Cowan and Reines [1]. Reactors are the largest terrestrial source of antineutrinos through the production of unstable fission fragments. These fission fragments are neutron rich and, thus, will beta decay to stability producing antineutrinos. An average of six beta decays occurs per fission; thus, a 1 GW_{th} reactor will produce $\mathcal{O}(10^{20})\bar{\nu}/\,\mathrm{sec}$. The vast majority of reactor nuclides lighter than uranium are generated directly as a fission product or by the beta decays of fission products, for instance

$$^{99}\mathrm{Zr} \rightarrow {}^{99}\mathrm{Nb} \rightarrow {}^{99}\mathrm{Mo} \rightarrow {}^{99}\mathrm{Tc}, \tag{1}$$

where we have truncated the chain at ^{99}Tc as its half-life of $\sim 2 \times 10^5$ yr allows us to consider it stable. Here, the daughter nuclides are produced from decays of their parents, which are dominantly produced via fissions. Thus, the decay rates of both the daughters and parents in the chain are linearly dependent on the fission rates. Equivalently, these nuclides are said to be linear in the neutron flux ϕ as the fission rate goes as $\phi\Sigma_{\mathrm{fiss}}$ for a macroscopic fission cross section Σ_{fiss}. A second mechanism for antineutrino production is from neutron captures on certain isotopes, such as

$$^{99}\mathrm{Tc} + n \rightarrow {}^{100}\mathrm{Tc}, \tag{2}$$

where the neutrons are the prompt neutrons from fission, thermalized by the moderator. Nuclides that are primarily produced via neutron captures require two neutrons: one to initiate the fission whose fission products result in a beta decay chain yielding the capture isotope, ^{99}Tc in the above example, and a second neutron for the actual neutron capture. Thus, naively, one would conclude that the production of ^{100}Tc is *quadratic* in the neutron flux. Thus, these nuclides will be produced in different quantities for different values of ϕ even if ϕT_{irr} is kept constant; we therefore name these nonlinear nuclides. This Letter examines how many such nonlinear nuclides with a relevant antineutrino yield exist and how large the resulting correction to the antineutrino spectrum can become.

To be a relevant nonlinear nuclide N, several conditions have to be met: (i) A large cumulative fission yield, Z_P of the capture isotope P. (ii) A large neutron capture cross section σ_P^c. (iii) The nonlinear nuclide must decay sufficiently quickly, that is, the decay constant λ must be large enough. (iv) The beta decay of the nonlinear nuclide has to have an end point above the inverse beta decay threshold of 1.8 MeV.

There are approximately 20 candidate nuclides fulfilling these conditions. An example of a relevant nonlinear nuclide, ^{100}Tc, is given in Fig. 1.

Here, ^{100}Tc is the beta-decaying nonlinear nuclide N and it is fission blocked from the beta decay chain by its stable isobar ^{100}Mo. Thus, ^{100}Tc is practically absent from fission products; i.e., its fission yield Y_f is negligible. Being fission blocked by a double-beta decay isotope, like ^{100}Mo, is characteristic for all candidates. The N production is then primarily governed by its precursor nuclide P, in this case ^{99}Tc. Furthermore, ^{99}Tc is relatively stable and linear as it is fed through its own decay chain meaning that, with a large enough cumulative yield and neutron capture cross section, the production of ^{100}Tc may be nonnegligible. To simplify our discussion, we consider only N that have stable precursors P (including ^{100}Tc), are significantly blocked ($Y_N^f \ll 1$), and have a significant feeder

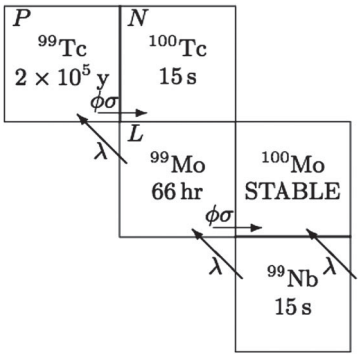

FIG. 1. Example of a typical nonlinear beta-decaying nuclide (N), ^{100}Tc. Half-lives taken from ENSDF [2].

cumulative yield ($\sum_{f=1}^{N_f} Z_P^f \geq 0.025$), where we used the JEFF-3.1 [3] fission yields. With these criteria we are able to reduce our list to four major nonlinear nuclides listed in Table I. Note that ^{100}Tc, ^{104}Rh, ^{110}Ag show predominantly ($> 95\%$) allowed Gamow-Teller decays, whereas ^{142}Pr exhibits a nonunique forbidden decay, which as we will see later, contributes less than 10% to the total nonlinear correction.

From Fig. 1 it is apparent we must solve a set of three linearly coupled nonhomogeneous differential equations, the Bateman equations [6], in order to express the abundance of N in terms of the thermal neutron flux ϕ and the irradiation time T_{irr}. Similar sets have been solved, without the neutron component, as an eigenvalue problem [7] and recursively [8].

The limiting cases of the solutions can be identified from the information provided in Table I. For irradiation times larger than the longest involved half-lives, which generally occur for the long-lived precursor parent L, and the relevant half-lives range from 0.57 to 39.3 d, we can assume that the isotope L is in equilibrium.

Once L has reached equilibrium, the next concern is that capture directly from the long-lived nuclide to a stable isotope can prevent the production of the neutron capture isotope. The decay rate $\ln 2/\tau_{1/2}$ of the long-lived nuclide equals the capture rate for a neutron flux density $\tilde{\phi}$ of

$$\tilde{\phi} = \frac{\ln 2}{\tau_{L\,1/2}} \sigma_L^c, \tag{3}$$

using the values given in Table I this yields a range of $\tilde{\phi} = 9 \times 10^{15}$–$2 \times 10^{18}$ s^{-1} cm^{-2}, which is nearly an order of magnitude above the values found for any of the reactors considered here. Thus, we conclude that this mechanism can practically be neglected. Note that for ^{136}Cs, the neutron capture on ^{135}Xe with a cross section of 2.7 Mb prevents any significant production.

The decay rate of the antineutrino producing nonlinear nuclide is large with half-lives in seconds to hours range and thus will be always in equilibrium with its much slower production rate. Therefore, for irradiation times which are long compared to the half-lives of L, the production rate of the nonlinear nuclide, which is the same as its decay rate is given by

$$\Gamma_{\mathrm{nonlinear}} \propto \underbrace{\Sigma_{\mathrm{fiss}} \phi Z_P T_{\mathrm{irr}}}_{\text{atoms of } P} \sigma_P^c \phi \propto T_{\mathrm{irr}} \phi^2, \tag{4}$$

hence, the name nonlinear nuclide. The decay rate of a fission product in equilibrium is given proportional to ϕ and thus the relative contribution of a nonlinear nuclide scales as $T_{\mathrm{irr}}\phi$. From Eq. (4) and Table I we also can conclude that ^{104}Rh will have the largest contribution for the fissile isotopes investigated, for fission of ^{235}U the second most important nonlinear nuclide is ^{100}Tc, whereas for the fission of both plutonium isotopes the second largest contribution stems from ^{110}Ag. We note, that reactors with a high neutron flux density and very long core lifetimes, in principle, can exhibit corrections in the (5–10)% range. In one example, assuming a neutron flux density of 10^{15} cm^{-2} s^{-1}, a power of 165 MW$_{\mathrm{th}}$, and five years of irradiation we find, through the analytical method of Eq. (5), a 4% correction during the last six months of operation. Clearly, naval reactors fulfill these characteristics and a precise measurement of the nonlinear correction to their antineutrino emissions may allow us to draw

TABLE I. Properties of the four selected nonlinear nuclides (N) including their beta end points (MeV), half-lives (sec), cumulative precursor (P) fission yields (atoms per fission), and their precursor flux-averaged thermal neutron capture cross section (b) taking the thermal flux from Fig. 3 of Ref. [4] and the cross sections from CINDER [5]. Also provided are the long-lived feeder parent (L) neutron capture cross sections and half-lives.

		^{100}Tc	^{104}Rh	^{110}Ag	^{142}Pr
N E_0 (MeV)		3.2	2.4	2.9	2.2
N $\tau_{1/2}$ (sec)		15.5	42.3	24.6	68 830
P Cumul. Fission Yields (atoms per fission)	^{235}U	0.061	0.031	0.000 29	0.059
	^{239}Pu	0.062	0.069	0.017	0.052
	^{241}Pu	0.056	0.065	0.030	0.049
P σ_P^c(b)		17.0	127	80.9	6.53
L $\tau_{1/2}^L$(d)		2.75	39.3	0.57	32.5
L σ_L^c(b)		1.57	7.08	18.2	26.7

conclusions about some of the design characteristics, like core size and operational history.

We can formulate an explicit solution for the nonlinear nuclides by solving the corresponding set of Bateman equations. The long-lived nuclide is dominantly produced via fission and destroyed through its neutron captures and decays. The precursor is produced via fission and decays from L. It is destroyed by neutron captures. Finally, the nonlinear nuclide is produced solely through captures on P and is destroyed via its own decays. Therefore, our nonlinear set is given by

$$\begin{aligned}\frac{dN_L}{dT_{\rm irr}} &= \vec{Z}_L \cdot \vec{\mathcal{F}} - \tilde{\lambda}_L N_L, \\ \frac{dN_P}{dT_{\rm irr}} &= \vec{Y}_P \cdot \vec{\mathcal{F}} + \lambda_L N_L - \phi\sigma_P^c N_P, \\ \frac{dN_N}{dT_{\rm irr}} &= \phi\sigma_P^c N_P - \lambda_N N_N, \end{aligned} \tag{5}$$

where $\tilde{\lambda}_i = \lambda_i + \phi\sigma_i^c$, $\vec{\mathcal{F}}$ is the fission rate vector, and $\vec{Z}_i$ ($\vec{Y}_i$) is the cumulative (individual) fission yields. All nuclear parameters are denoted by their subscript. It is straightforward to solve Eq. (5) analytically, but the salient features are contained in the above description of the limiting cases. Many of the reactor physics effects neglected in the simplified reaction network used result in non-negligible corrections and we find that the analytic result generally is within a factor of 2 the solution derived from using a full reaction network. The full reaction network is evaluated using the standardized computer analyses for licensing and evaluation (SCALE-6.1) [9] reactor simulation suite, developed by Oak Ridge National Laboratory.

Now that we have an expression for the activity of these four nonlinear beta-decaying nuclides we can apply a neutrino spectrum to each decay to generate a neutrino rate. The neutrino spectra are applied to our four nuclides following Ref. [10], which generates the neutrino spectra for each nonlinear nuclide. The neutrino spectra were then summed to determine the total nonlinear correction.

Solving Eq. (5) will lead to an expression for the activity of the nonlinear nuclides, which can be combined with the spectra of each nonlinear isotope to produce the total nonlinear spectral contribution. Comparing this with the total reactor spectra shows that the nonlinear spectra falls off steeply at ~2.4 MeV. This nonlinear spectral contribution is important as it interferes with other low-energy corrections, such as the spent fuel signal [11], the nonequilibrium correction for inverse beta decay experiments which has been evaluated in Ref. [12], where neutron capture was specifically neglected. For elastic antineutrino-electron scattering experiments at very low energies a detailed discussion of the nonequilibrium correction including some neutron captures (different than those considered here) can be found in Refs. [13,14]. All of these corrections, including the nonlinear correction, will directly impact geoneutrino searches [15,16] wherever a sizable reactor signal needs to be subtracted, as, for instance, in the Jiangmen Underground Neutrino Observatory [17].

Using SCALE, we are able to model nine different reactor configurations, spanning 3 orders of magnitude in their thermal neutron flux. The first is a natural uranium loaded and graphite-moderated reactor, similar in design to the British Calder-Hall reactor. This reactor is referred to as the 5 MW_e reactor and has been previously modeled [18]. The next reactor uses natural uranium as fuel and heavy water as a moderator, similar in design to the Canada Deuterium Uranium Reactor. This reactor, referred to as the IR40, has also been previously modeled [19]. The third reactor is fueled with low-enriched uranium (LEU) with a water moderator. These reactors are pressurized water reactors (PWR) similar in design to the Daya Bay cores. The Daya Bay reactors have also been previously modeled to estimate the spent fuel contribution [20]. The PWR cores are simulated using a three-batch method, where a full core consists of three parts: a third each of fresh, once-irradiated, and twice-irradiated fuel. We also include a single-batch calculation for comparison. Next, we simulate a research reactor, named the IRT reactor, which is a pool-type reactor using highly enriched uranium (HEU) fuel elements, natural uranium target elements, and water as a moderator. It was previously simulated, also in Ref. [18]. We have also recreated the measurements conducted at the ILL reactor, irradiating a fissile mass with a specific neutron flux according to Refs. [21–23]. Finally, we simulate the High Flux Isotope Reactor (HFIR) at Oak Ridge National Laboratory, which represents the highest steady-state neutron flux commercially available. Our simulation closely follows that of Ref. [24]. This reactor database spans over 3 orders of magnitude for the neutron fluxes and we aim to find a nonlinear correction trend as a function of ϕ. Each reactor is irradiated with its own typical power history using the SCALE simulation suite. The burn-up and reactor specifications are given in Table II.

We use the ORIGEN depletion subroutine to compute the fission rates and nuclide activities as a function of irradiation time. We use the linear antineutrino yields for ^{235}U, ^{239}Pu, and ^{241}Pu from Ref. [10] and for ^{238}U from Ref. [12] to convert the fission rates to a total neutrino spectrum for each reactor during its power cycle. The nonlinear correction is isolated by selecting the activities of our four nonlinear nuclides and converting these into a neutrino spectrum using the beta decay description in Ref. [10]. Each spectrum is binned into 250 keV bins and a nonlinear correction is determined from the ratio of the nonlinear contribution to the total reactor spectrum at all irradiation times. This result is then used to calculate a time-averaged nonlinear correction, shown in Fig. 2.

TABLE II. Details of the reactor calculations via ORIGEN including the burn-up, thermal neutron flux, and design details. Calculations for the ILL reactor mimic the original Schreckenbach *et al.* measurements and show no nonlinear contamination.

	PWR						ILL or Schreckenbach *et al.*		
	5 MW_e	IR40	1-batch	3-batch	IRT	HFIR	^{235}U	^{239}Pu	^{241}Pu
Fuel and moderator	NU + C	NU + D_2O	LEU + H_2O		HEU + H_2O	HEU + H_2O	HEU + D_2O		
Burn-up [MWd/t]	32380	31200	31510	26110	2230	2550	7.3×10^{-5}	1.1×10^{-4}	1.7×10^{-4}
ϕ[n/cm^2/ sec]	1.6×10^{12}	3.6×10^{13}	4.4×10^{13}	4.4×10^{13}	1.5×10^{14}	2.5×10^{15}	3.3×10^{14}	3.3×10^{14}	3.3×10^{14}
Max[$\langle \Phi_{NL}/\Phi_R \rangle_T$] [%]	0.027	0.15	0.24	0.92	0.11	0.10	3.1×10^{-5}	2.6×10^{-3}	4.7×10^{-3}

With this nonlinear low-energy neutrino correction, we can see that commercial reactors can be very sensitive to the resulting effects, where it becomes comparable with spent fuel [$\sim$(1–2)%] [11] and the nonequilibrium correction [$\sim$(1–4)%] [13,14]. Therefore, neutrino experiments will need to consider the nonlinear correction when predicting the total reactor neutrino spectrum, especially in the low energy region where detailed reactor simulations are necessary. Verification of this new correction could, in principle, be accomplished by measuring the abundance of the nonlinear nuclide beta-decay daughters, which are stable (^{100}Ru, ^{104}Pd, ^{110}Cd, and ^{142}Nd). A final item of note is that the widely used measurements of the cumulative beta spectra from fissions of ^{235}U [21], ^{239}Pu, and ^{241}Pu [23], and now ^{238}U [22] have utilized research reactors with fluxes of $\mathcal{O}(10^{14}$ n/cm^2/ sec). Our analysis has been conducted to reproduce the measurements by Schreckenbach *et al.* to determine if nonlinear effects appear in these measurements. A flux of $\phi = 3.3 \times 10^{14}$ n/cm^2/ sec was used with irradiation times of 12, 36, 43, and 42 hr for ^{235}U, ^{239}Pu, ^{241}Pu, and ^{238}U, respectively, in accordance with Refs. [21–23,25,26]. The results for these calculations, shown in Table II, illustrate that these measurements are not contaminated by nonlinear corrections and thus the extracted neutrino fluxes [10,12] are unaffected. The actual spectra of the nonlinear correction can be obtained from [27].

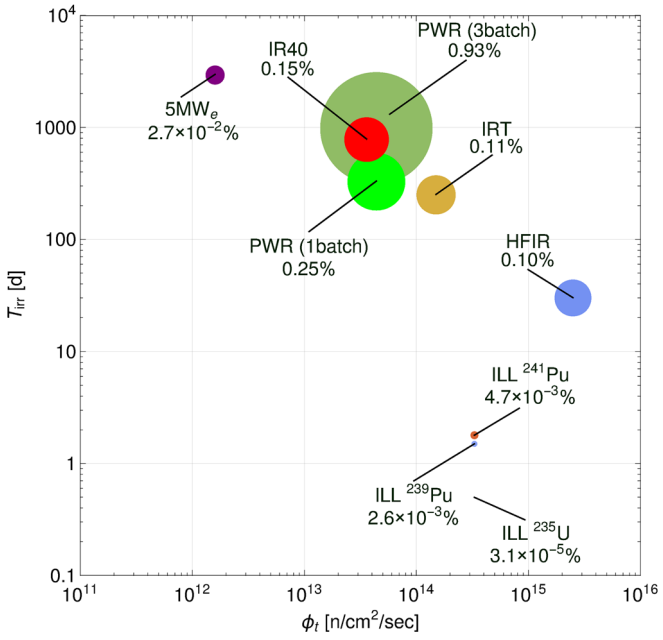

FIG. 2. Time-averaged maximum nonlinear correction for nine different reactor configurations as computed via SCALE. Both a single batch and a 3-batch core were considered for the PWR. Area of the disk is proportional to the size of the correction.

The lack of nonlinear corrections in the Schreckenbach measurements is due to the short irradiation times T_{irr}, which are all less than two days. As we have noted earlier, such as in Fig. 1, most of our nonlinear nuclides are fed via a precursor nuclide P with a long-lived parent L. The large half-lives, relative to T_{irr}, of the L nuclides prevents the buildup of the feeder nuclides, which then prevents the buildup of the nonlinear nuclides, thus preserving the Schreckenbach measurements. This same effect is seen in the diminished nonlinear correction for the HFIR reactor, which involves irradiation cycles less than 30 d. Two nonlinear nuclides (^{104}Rh and ^{142}Pr) are fed through an L with $\tau_{1/2} \geq 30$ d, so their contribution to the HFIR correction is lower than would be expected for longer irradiation times.

In our note we have introduced a new low-energy correction to the reactor antineutrino spectrum. This correction is due to nonlinear nuclides in the reactor, which are dominantly produced via neutron captures. Demanding that our nuclides of interest meet several criteria, we have limited the list of these nonlinear nuclides to four that can impact neutrino studies: ^{100}Tc, ^{104}Rh, ^{110}Ag, and ^{142}Pr. We derived an analytic solution for the abundance of these nuclides in a reactor environment, which depends on the neutron flux in a nonlinear fashion. We calculated the nonlinear corrections for several reactor designs spanning thermal neutron fluxes from $\mathcal{O}(10^{12}$ n/cm^2/ sec) to $\mathcal{O}(10^{15}$ n/cm^2/ sec), discovering a nonlinear neutrino excess as large as $\sim$1%. The resulting nonlinear nuclide production is negligible for short irradiation times less than 30 d, but much larger for multibatch commercial reactors, which can reach large burn-up values. This result indicates that special attention should be given to the nonlinear correction in future neutrino experiments, requiring detailed reactor simulations to correctly predict this excess.

We would like to thank A. Hayes for the many discussions on nonlinear nuclide production in a reactor as well as D. Ilas and the ORNL team behind the maintenance and verification of SCALE. This work was supported by the U.S. Department of Energy under Award No. DE-SC0013632.

*pahuber@vt.edu
†pjaffke@vt.edu

[1] C. Cowan, F. Reines, F. Harrison, H. Kruse, and A. McGuire, Science **124**, 103 (1956).
[2] J. Tuli, Evaluated nuclear structure data file, http://www.nndc.bnl.gov/ensdf/.
[3] A. Koning, R. Forrest, M. Kellett, R. Mills, H. Henriksson, and Y. Rugama, Joint evaluated fission and fusion file, incident-neutron data, http://www-nds.iaea.org/exfor/endf00.htm.
[4] Department of Energy, *Nuclear Physics and Reactor Theory Module 2: Reactor Theory (Neutron Characteristics)*, Vol. 1 (National Technical Information Services, Springfield, VA, 1993).
[5] W. Wilson, T. England, and M. Brady, CinderLibrary, https://rsicc.ornl.gov/codes/ccc/ccc7/ccc-755.html.
[6] H. Bateman, Proc. Cambridge Philos. Soc. **15**, 423 (1910).
[7] L. Moral and A. F. Pacheco, Am. J. Phys. **71**, 684 (2003).
[8] J. Cetnar, Ann. Nucl. Energy **33**, 640 (2006).
[9] ORNL, Standardized computation and licensing evaluation, http://scale.ornl.gov/.
[10] P. Huber, Phys. Rev. C **84**, 024617 (2011); **85**, 029901(E) (2012).
[11] B. Zhou, X.-C. Ruan, Y.-B. Nie, Z.-Y. Zhou, F.-P. An, and J. Cao, Chin. Phys. C **36**, 1 (2012).
[12] T. A. Mueller *et al.*, Phys. Rev. C **83**, 054615 (2011).
[13] L. Mikaelyan, Phys. At. Nucl. **65**, 1173 (2002).
[14] V. Kopeikin, Phys. At. Nucl. **66**, 472 (2003).
[15] O. Sramek, W. F. McDonough, and J. G. Learned, Adv. High Energy Phys. **2012**, 235686 (2012).
[16] G. Domogatski, V. Kopeikin, L. Mikaelyan, and V. Sinev, Phys. At. Nucl. **68**, 69 (2005).
[17] R. Han, Y.-F. Li, L. Zhan, W. F. McDonough, and J. Cao, Chin. Phys. C **40**, 033003 (2016).
[18] E. Christensen, P. Huber, and P. Jaffke, Sci. Global Secur. **23**, 20 (2015).
[19] E. Christensen, P. Huber, P. Jaffke, and T. E. Shea, Phys. Rev. Lett. **113**, 042503 (2014).
[20] F. An *et al.* (Daya Bay Collaboration), Phys. Rev. Lett. **108**, 171803 (2012).
[21] K. Schreckenbach, G. Colvin, W. Gelletly, and F. Von Feilitzsch, Phys. Lett. B **160**, 325 (1985).
[22] N. Haag, A. Gütlein, M. Hofmann, L. Oberauer, W. Potzel, K. Schreckenbach, and F. M. Wagner, Phys. Rev. Lett. **112**, 122501 (2014).
[23] A. A. Hahn, K. Schreckenbach, W. Gelletly, F. von Feilitzsch, G. Colvin, and B. Krusche, Phys. Lett. B **218**, 365 (1989).
[24] D. Ilas, Report No. ORNL/TM-2011/367, Oak Ridge National Laboratory, 2012.
[25] K. Schreckenbach, H. Faust, F. von Feilitzsch, A. Hahn, K. Hawerkamp, and J. Vuilleumier, Phys. Lett. B **99**, 251 (1981).
[26] F. Von Feilitzsch, A. Hahn, and K. Schreckenbach, Phys. Lett. B **118**, 162 (1982).
[27] See Supplemental Material http://link.aps.org/supplemental/10.1103/PhysRevLett.116.122503 for the neutrino spectra used in the calculations.